Reducing Conservatism in Probabilistic Corrosion Analyses using Cluster Profiles

Daryl Bandstra[1], Alex Fraser[1], Miaad Safari[2], Kai Ji[2]
[1]Integral Engineering, [2]Enbridge Gas Inc.

Pipeline Pigging and Integrity Management Conference

February 12-16, 2024

Organized by
Clarion Technical Conferences

https://doi.org/10.52202/072781-0051

Proceedings of the 2024 **Pipeline Pigging and Integrity Management Conference**.
Copyright ©*2024 by* **Clarion Technical Conferences** *and* **the author(s)**.
All rights reserved. This document may not be reproduced in any form without permission from the copyright owners.

https://doi.org/10.52202/072781-0051

Abstract

The transmission pipeline industry is increasingly utilizing probabilistic models to assess the probability of failure of anomalies measured during in-line inspections, such as corrosion and cracks. PHMSA (Pipeline and Hazardous Materials Safety Administration) has recently classified probabilistic models as "Best Practice" and suitable for supporting all types of decision-making, as these models effectively represent the uncertainty in input data using probabilistic distributions. Examples of decision types are baseline integrity assessment, mitigative measure comparison, cost-benefit analyses for risk reduction options, and integrity assessment interval determination. When modelling corrosion using a probabilistic model, the in-line inspection provides measurements of individual corrosion anomalies. When these anomalies are in close proximity, there is potential for interactions that reduce the overall burst capacity, and the effect of these interactions can be considered by analyzing these individual anomalies together as a cluster.

Some probabilistic analyses idealize the clusters as single anomalies, while others address the added complexity of considering all possible combinations of the individual anomalies that comprise the cluster using a methodology called the Effective Area method. This presentation will investigate the differences in the estimated probability of failure of these two approaches by evaluating a range of test cases and real-world clusters. These cases illustrate scenarios where significant discrepancies exist and areas where both approaches yield comparable results.

Background

In the pipeline industry, operators utilize risk management programs to identify, analyze, and evaluate risks to the integrity of their pipeline system to support decision-making on risk treatment activities (e.g. repair). In many jurisdictions, national regulations and standards may require these programs, such as in the United States [1-2] and Canada [3].

In the US, operators are required to report significant incidents to the Pipeline and Hazardous Materials Safety Administration (PHMSA). PHMSA is an agency within the US Department of Transportation (US DOT) that is tasked with developing and enforcing regulations for the US pipeline transportation system and hazardous materials transport [4]. These accident reports include information about the pipeline, the cause of the failure, and the results of the accident. All accident reports are collected into publicly available datasets through the PHMSA website [5]. The total number of rupture incidents on gas transmission and hazardous liquids pipelines in the PHMSA dataset from 2010-2023, separated by corrosion and non-corrosion causes, is illustrated below in Figure 1. In this dataset, 32.5% of rupture incidents on gas transmission and 20% of rupture incidents on hazardous liquid pipelines were caused by corrosion. Evidently, corrosion is a significant integrity threat for both gas and hazardous liquid transmission pipeline systems.

https://doi.org/10.52202/072781-0051

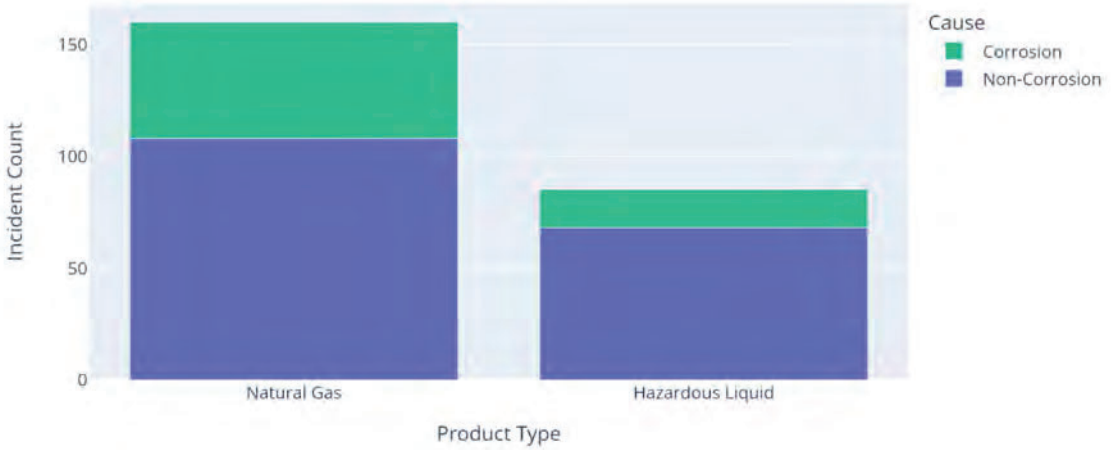

Figure 1. Count of rupture incidents on onshore transmission pipelines by cause and product type (PHMSA 2010-2023)

To manage the risk of corrosion, pipeline operators employ risk models that utilize a wide range of methodologies. A 2020 report by PHMSA categorized these risk model types into four categories [6]: Qualitative, Relative Assessment/Index, Quantitative System, and Probabilistic. This report defines probabilistic models as a "*Model with inputs that are quantities or probability distributions and with outputs that are probability distributions.*" This report further compared the suitability of different risk model types for supporting a variety of decision types. For decision types such as mitigative measure evaluation, cost-benefit analysis, and integrity assessment interval determination, the report concluded that Quantitative risk models are "Applicable" and Probabilistic models are "Best Practice."

For managing the risk of corrosion, probabilistic models are routinely used to assess probability of failure of anomalies measured during in-line inspection runs. The general approach is illustrated in Figure 2, where uncertain inputs are propagated through a physics-based structural model to assess the resulting probability of failure. In the domain of structural engineering, this approach may also be referred to as a "structural reliability" model.

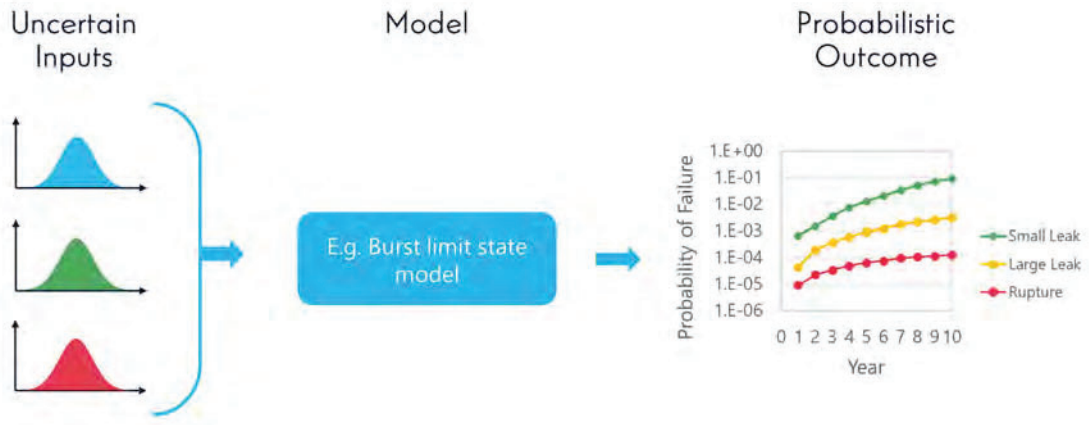

Figure 2. General overview of probabilistic structural reliability model

https://doi.org/10.52202/072781-0051

Within the pipeline industry, papers published in the mid-1990's describe early applications of structural reliability to pipeline corrosion [7-10]. The basic approach used in this early work is largely unchanged today and the majority of the developments in the following decades focused on making the approach to corrosion more comprehensive [11], increasing computational efficiency [12-14], characterizing the effect of maintenance actions [15], and evaluating the performance of different burst models [16-17]. Today, reliability methods have been applied by many major pipeline operators to manage risk and integrity. These methods have also been included in pipeline codes such as CSA Z662 [3] and ISO 16708 [18].

The probabilistic outcome illustrated in Figure 2 is obtained by solving a multi-dimensional integral, most commonly using Direct Monte Carlo simulation. DMC is a simple and robust methodology that uses random sampling to simulate a large number of experiments. DMC estimates the probability of failure based on the number of random simulations that fail a given limit state out of the total number of simulations. The major drawback of DMC is that it requires a large number of simulations, and therefore a large amount of computation time, to estimate small failure probabilities. This computation time can be reduced by parallelizing the simulations across multiple Central Processing Units (CPUs), but this approach requires additional resources, such as access to a high-performance computer or cloud computing platform.

Corrosion Limit States

The probabilistic model outlined in Figure 2 produces a value for the probability of failure, which requires a defined point of failure. This point of failure is defined by a mathematical equation called a *limit state function*. Multiple limit states are typically considered when assessing corrosion, as a corrosion anomaly can fail by modes such as small leak or burst. Furthermore, burst events can be separated into large leak and rupture failure modes, which can have significantly different consequences because of the different hole sizes and associated outflow potential. Figure 3, adapted from CSA Z662 [3], conceptually illustrates how the limit states vary for two independent random variables (depth and length). In practice, however, there are additional random variables to consider such as wall thickness and yield strength which increase the number of dimensions that define the limit state function.

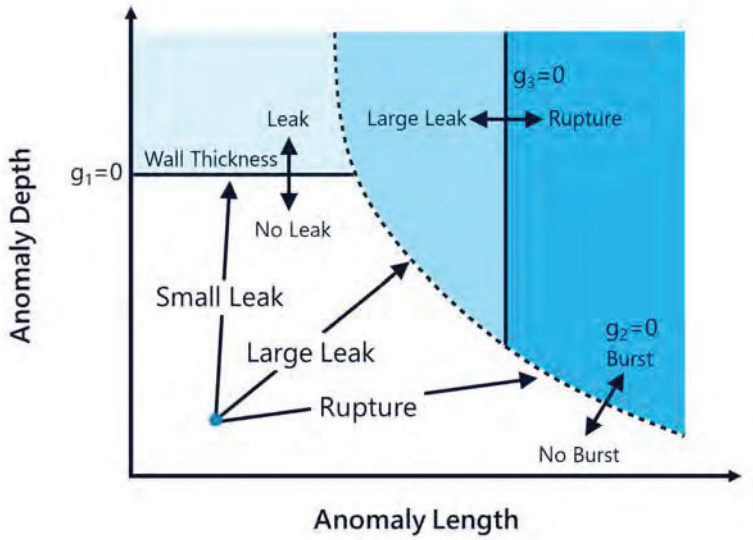

Figure 3. Corrosion Limit States from CSA Z662-23 Annex O (figure adapted from CSA Z662-23 Annex O)

https://doi.org/10.52202/072781-0051

Burst events (large leak or rupture) are often the primary concern as they have the largest potential safety consequence as that the gas outflow from a failed anomaly can ignite, resulting in a jet fire. The limit state equation for burst of a corrosion anomaly (g_2 line in Figure 3) is calculated in CSA Z662-23 Annex O as the difference between the estimated pressure resistance of an anomaly (including model error) minus the applied pressure load, as described below in Equation 1.

$$g_2 = r_a - P \tag{1}$$

where,

$r_a =$ the estimated pressure resistance including model error

$P =$ The internal pressure

The estimated pressure resistance is an equation (i.e. a function) that includes a term that compares the ratio of the anomaly average depth to the total wall thickness (d_a/t). This ratio (d_a/t) is equivalent to ratio of the removed area due to corrosion ($A_c=d_{avg}\cdot l$) over the total area before corrosion takes place ($A_0 = t\cdot l$) area.

$$r_a = f\left(\frac{1-\frac{d_a}{t}}{1-\frac{d_a}{M\cdot t}}\right) \tag{2}$$

where,

$r_a =$ the estimated pressure resistance including model error

$d_a =$ Anomaly depth

$M =$ The Folias factor

$t =$ Wall thickness

Corroded Area and Interaction

An operator may not have a measurement of the average depth, as many in-line inspection tools may only report the maximum depth and total length of the anomaly. The most conservative approach would be to assume all of the material down to the maximum depth has corroded away along the entire length of the anomaly, as illustrated by the rectangular box profile in Figure 4. Common deterministic models assume the shape of the corroded area. For example, ASME B31G uses a semi-elliptical shape where 2/3 of the box area is removed and ASME B31G Modified uses a ratio of 0.85. CSA Z662-23 Annex O references a distribution from Kiefner and Vieth [19] where the mean value is 0.48 and the variation is quantified for use in probabilistic methods.

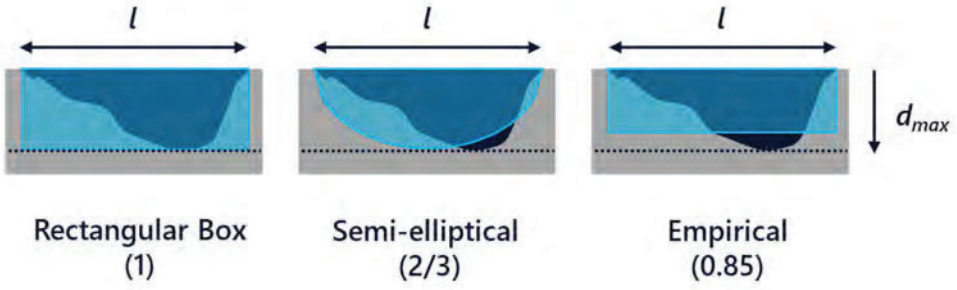

Figure 4. Corroded area assumptions for selected corrosion burst models

https://doi.org/10.52202/072781-0051

When multiple anomalies are located in closely spaced proximity, the stress fields interact and have the potential to decrease the failure pressure compared to a situation where these anomalies are isolated (i.e. far apart). To consider these interactions, an analysis could represent the cluster as a single anomaly with a maximum depth equal to the maximum depth of any anomaly in the cluster and a length equal to the total length of the cluster. The assumption is illustrated by the black dotted rectangle in Figure 5. A burst model such as a ASME B31G or ASME B31G Modified would then calculate the corroded area based on this maximum depth and total length. In this case, the actual corroded area is much lower than these burst models would assume due to the combination of a single deep anomaly with two shallow anomalies.

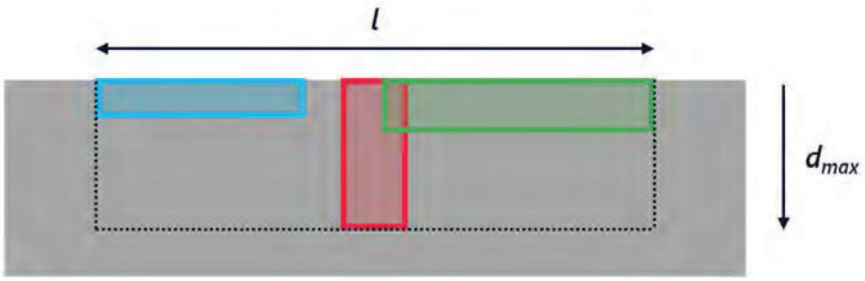

Figure 5. Illustrative Cluster with three individual metal loss anomalies

To reduce the conservatism introduced in scenarios such as this, the Effective Area Method was developed to assess the actual corroded area [20]. This method involves assessing all possible combinations along the profile to determine the effective area of the critical section. An illustration of both methods is shown below in Figure 6. To summarize, two potential approaches for assessing a set of interacting anomalies (i.e. a cluster) are

- Single Anomaly – model as a single anomaly with maximum depth and full cluster length
- Effective Area – model all combinations to directly assess the critical corroded area.

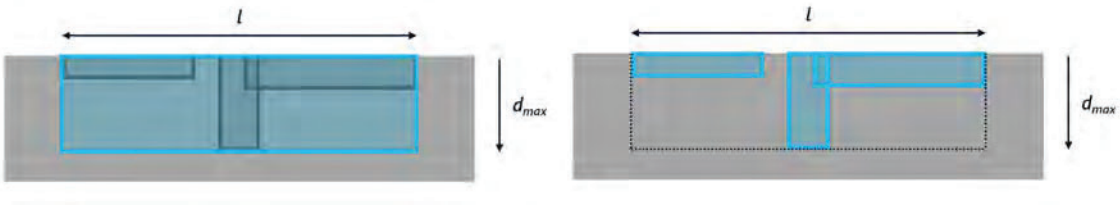

a.) Cluster as single anomaly b.) Effective Area Method

Figure 6. Illustration of two approaches to characterizing the Cluster

In a probabilistic model utilized in this study, the Effective Area method was implemented using the process outlined in Figure 7. In this implementation, the uncertainty in the depth and length of each anomaly is defined by the ILI tool measurement error. During the first simulation, the measurement error is used to sample possible defect sizes. Then the Effective Area algorithm is applied to these sampled sizes to determine the critical combination of anomalies that returns the lowest burst pressure. Then, this critical combination of anomalies is used to assess the time to failure. The results are saved and the algorithm proceeds to the next simulation. This process would repeat until the specified total number of simulations is reached (e.g. 1 million).

https://doi.org/10.52202/072781-0051

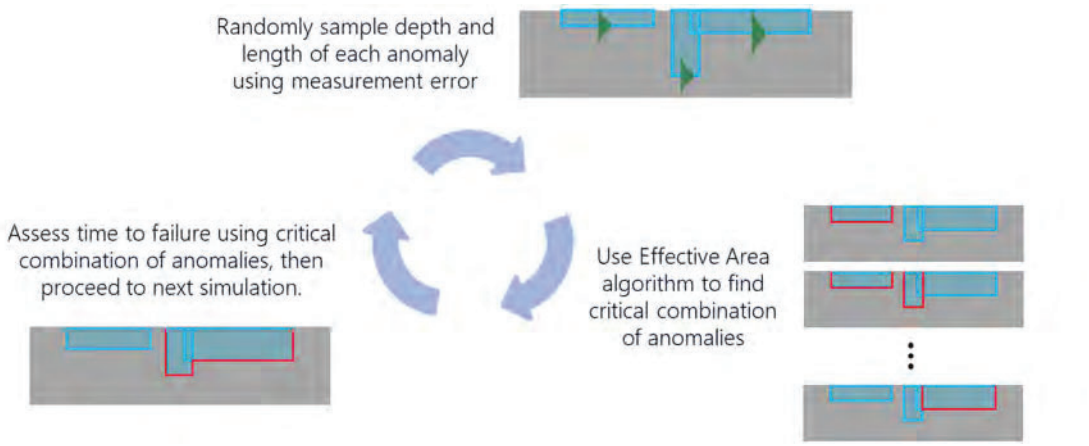

Figure 7. Illustrative Cluster with three individual metal loss anomalies

As the number of anomalies in the cluster increases, the number of combinations that must be assessed using the Effective Area method increases significantly. In a probabilistic analysis that uses Direct Monte Carlo to assess the probability of failure, this Effective Area process must be repeated in each simulation, which may be 1 million times or more! Therefore, the computational effort (time/cost) of assessing clusters in a probabilistic analysis using the Effective Area method can become very large compared to the approach where the cluster is a modelled single anomaly. In summary, modeling the cluster as a single anomaly introduces conservatism into the assessment which can be reduced using the Effective Area method; however, the Effective Area method can significantly increase the computational effort required to assess the cluster. One of the primary aims of this study is to investigate the costs and benefits associated with using the more refined Effective Area method

Overview of Analysis

The objective of the analysis presented in this study was to utilize a real-world dataset of inspected anomalies to compare the computational effort and probabilities of failure for clusters that were analyzed using each of the two methods (Single Anomaly and Effective Area). In general, the clusters evaluated using the Effective Area method are expected to have a similar or lower probability of failure at the cost of more computational effort to obtain the result.

The dataset used in this was provided by Enbridge Gas Incorporated (Enbridge) and contained measurements of 27,756 individual corrosion anomalies measured during in-line inspections on a range of transmission pipelines. Each of the anomalies was located close enough in the longitudinal or circumferential direction to be clustered with one or more adjacent anomalies on the pipeline. In total, the set of anomalies was clustered into 10,319 unique clusters. To visualize the distribution of cluster sizes, a histogram illustrating the count of clusters that contain a particular number of anomalies is shown below in Figure 8. The histogram illustrates that the majority of clusters only contain a few anomalies and that clusters containing a large number of (e.g. 10 or more) are rare. Around 73% of the clusters contained only two anomalies and only 1% of the clusters contained more than 10 anomalies in a single cluster. The dataset's largest cluster (by anomaly count) contained 151 individual anomalies.

https://doi.org/10.52202/072781-0051

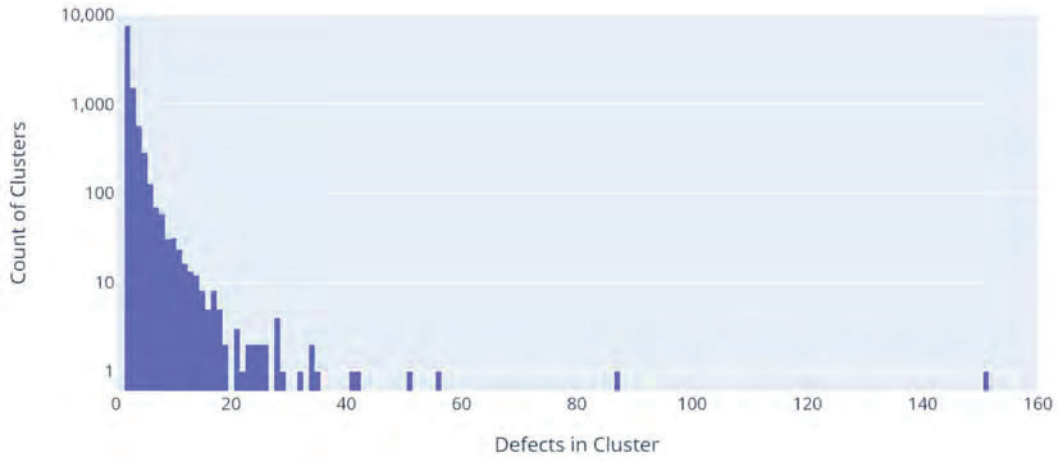

Figure 8. Histogram of count of clusters by number of anomalies in cluster

The analysis algorithm and input assumptions used in this study were developed by Integral Engineering specifically for this study and have differences from the probabilistic model implementation and standard assumptions used in practice by Enbridge. As such, the probabilities of failure produced for this analysis are realistic in nature but differ from the actual values used for decision-making at Enbridge. The input distributions for each anomaly were defined primarily using Enbridge pipeline records and distributions from CSA Z662-23 Annex O. A full list of the assumed input distributions is provided in Table 1. The limit state equations for corrosion were also adopted from CSA Z662-23 Annex O, including the associated model error distribution. For simplicity of comparison, all anomalies were assumed to have been measured at the current date, and the probability of failure in each future year was calculated for each failure mode (small leak, large leak, and rupture).

Table 1. Probabilistic input parameter distributions

Parameter	Distribution	Mean	Standard Deviation	Source
Diameter	Normal	1 x Outer Diameter	0.0006 x Mean	CSA Z662-23 Annex O
Wall Thickness	Normal	1.01 x Nominal	0.01 x Mean	CSA Z662-23 Annex O
Pressure	Deterministic	1 x MAOP		Pipeline Records
Yield Strength	Normal	1.1 x SMYS	0.035 x Mean	CSA Z662-23 Annex O
Tensile Strength	Normal	1.12 x SMTS	0.035 x Mean	CSA Z662-23 Annex O
Maximum Anomaly Depth	Normal	Reported Depth	ILI Vendor Specified Error	Inspection Records
Anomaly length	Normal	Reported Length	ILI Vendor Specified Error	Inspection Records
Max.-to-Avg. Depth Ratio	Shifted Lognormal (Shift=1)	2.08	1.04	CSA Z662-23 Annex O
Maximum Depth Growth Rate	Growth by Rule	50% of Age		Wright et al. 2018
Model Error				CSA Z662-23 Annex O

https://doi.org/10.52202/072781-0051

Each cluster was simulated using 10^6 simulations and the results for a single example cluster are shown below in Figure 9.

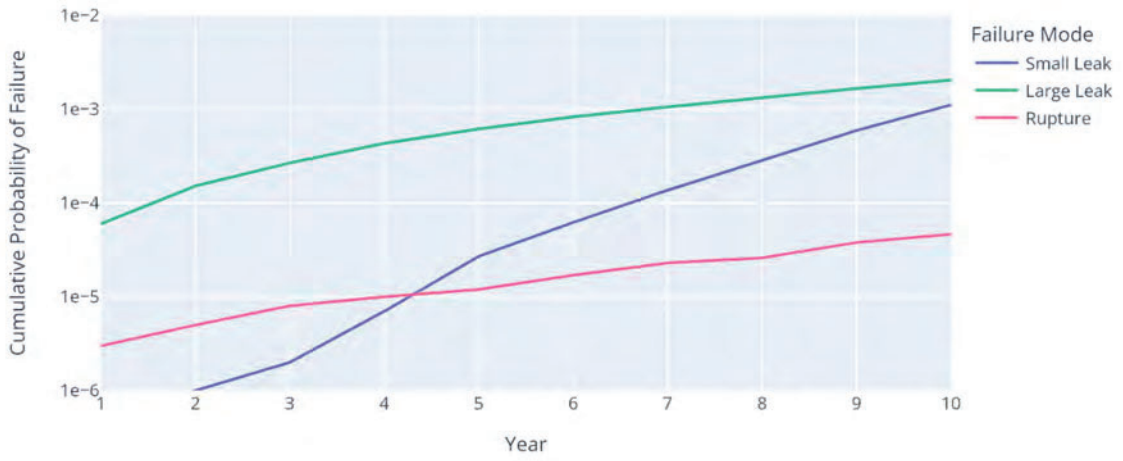

Figure 9. Example probability of failure results for a single cluster

Investigation of Computation Effort

As the Effective Area Method requires the algorithm to check every combination of profiles created by the anomalies in the cluster, the computational effort is increased over the Single Anomaly method. To investigate the real-world increase in computational effort, the computational run-time required to complete the 10^6 simulations was tracked during the analysis of the full set of clusters in this study. The ratio of the increase in time required to complete the analysis using the Effective Area method over the Single Anomaly method was calculated for clusters with different numbers of anomalies, and the results are shown in Figure 10. A cluster with 10 anomalies required 13 times more run-time than a single anomaly, while a cluster with around 100 anomalies required around 1000 times more run-time than a single anomaly. This result illustrates that the Effective Area method can significantly increase the computational effort for clusters with a large number of anomalies. For example, suppose the analysis of a cluster comprised of 150 individual anomalies takes 1 minute to calculate (when modelled using the Single Anomaly method). Based on the curve shown in Figure 10, the analysis of the cluster using the Effective Area method will take 3000 minutes, or just over 2 days. This run-time can be reduced by parallelizing the simulations using a platform such as cloud computing; however, this still equates to an increase in analysis cost of 3000 times more than the Single Anomaly method.

Note that the shape of this curve is highly dependent on the specific implementation of the Monte Carlo simulation procedure. Choices such as the specific programming language, coding structure, and use of optimizations can significantly affect the run-time. These results are provided to illustrate a real-world example; however, any given implementation would be expected to vary from these results.

https://doi.org/10.52202/072781-0051

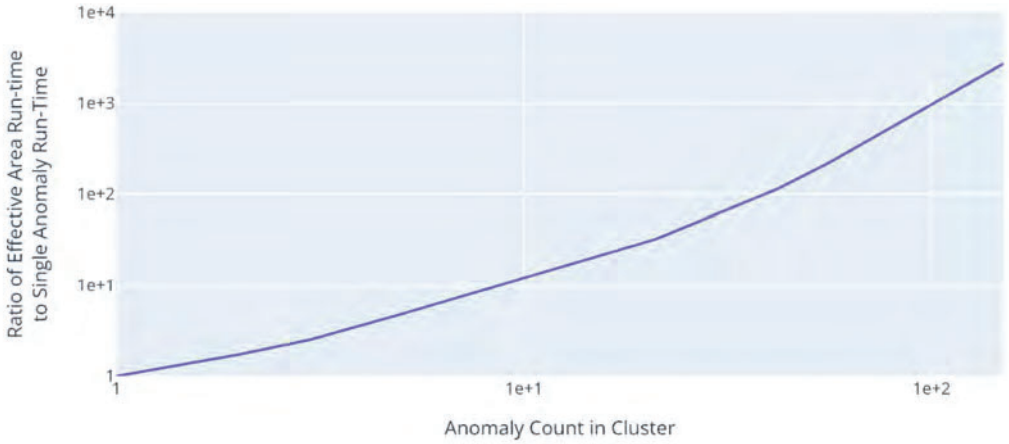

Figure 10. Ratio of run-time in this study for clusters using effective area method vs. single anomaly method

The results of the curve shown in Figure 10 can be used to determine the effective increase in computational effort required to complete the analysis of all clusters in the dataset. The results of the total run-time for the cluster population are shown in Figure 11, where the Effective Area method for all clusters takes around 3 times as long to run as the Single Anomaly method. As most clusters contain a low number of anomalies (e.g. 2 or 3), the increase in computational effort is relatively small (e.g. 2 times more than a single anomaly). For a few clusters, such as the cluster with 151 anomalies, the computational effort is increased by more than 3000 times; however, clusters with this many anomalies are rare in the dataset.

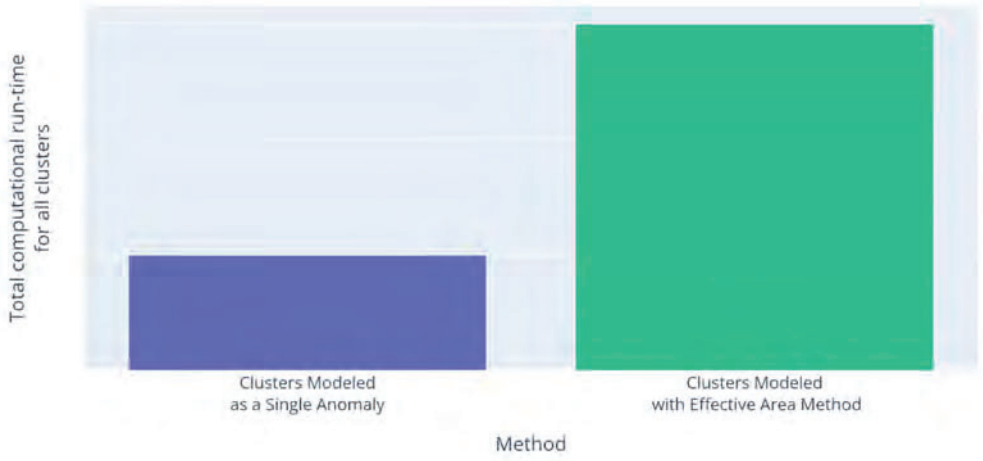

Figure 11. Run-time in this study for clusters using effective area method vs. single anomaly method

https://doi.org/10.52202/072781-0051

Investigation of Change in Probability of Failure

The results of the previous section quantify the costs associated with using either method. This section investigates the benefit, in terms of a reduction in probability of failure that is gained when using the Effective Area method over the Single Anomaly method. Burst failures (large leak or rupture failures) have the largest potential for life safety consequences, therefore the probability of burst failure results were the focus of this investigation. The annual probability of burst failure in Year 7 was selected as the primary metric for analysis as this represents a typical time before the next in-line inspection, at which point an operator would re-measure the anomalies. A scatter plot comparing the results obtained by two methods (Single Anomaly vs Effective Area) is shown below in Figure 12. A "unity" line where the two methods produce the same result is drawn diagonally in black. Points that lie above the black line are clusters where the Single Anomaly method produced a higher probability of burst than the Effective Area method. In general, the Single Anomaly method produces a higher probability of burst failure than the Effective Area method, by up to three orders of magnitude for some clusters. For some clusters near the lower simulation limit (10^{-6}), the Single Anomaly method did produce a lower probability of burst failure than the Effective Area method; however, the Monte Carlo estimator error becomes more significant near the lower limit causing some additional scatter.

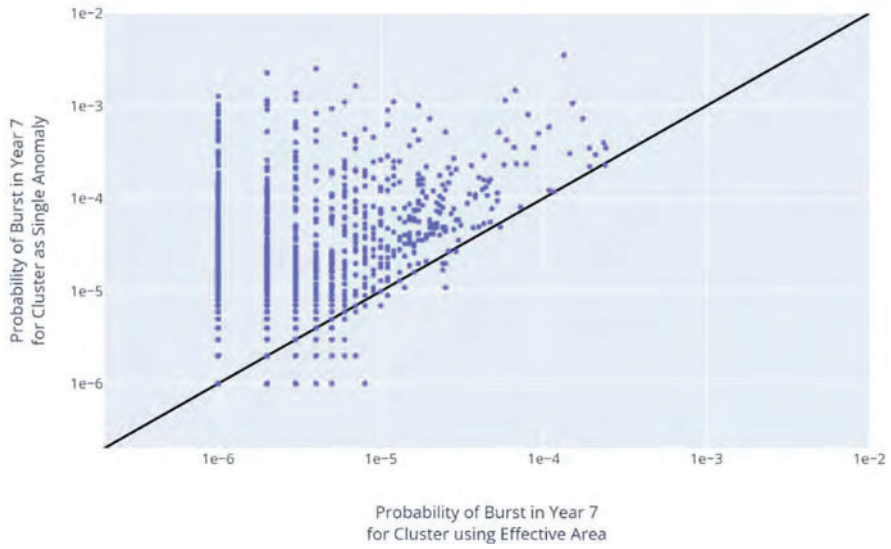

Figure 12. Comparison of probability of burst failure in Year 7 for single anomaly vs. effective area

https://doi.org/10.52202/072781-0051

For each cluster, the ratio of the probability of burst result from the Single Anomaly method to the Effective Area method was calculated. A histogram of these results is shown below in Figure 13. Most clusters have a probability of burst that is reduced by 1 to 10 times; however, the probability of burst for some clusters may be reduced by 100 or even 1000 times.

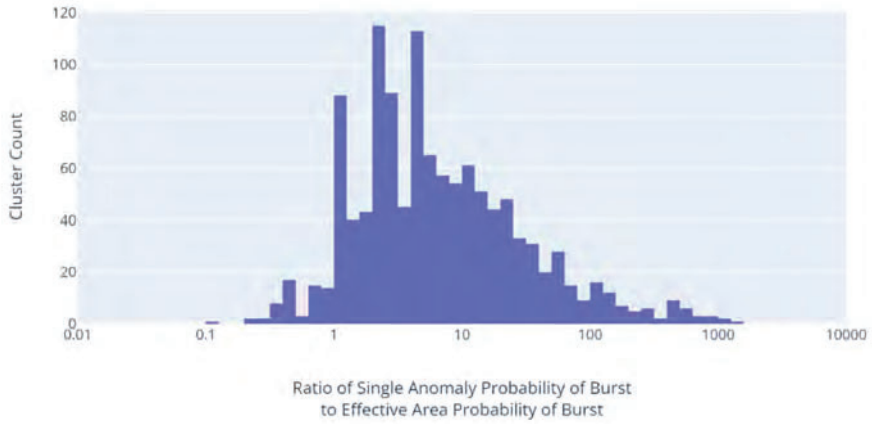

Figure 13. Histogram of ratio of burst probabilities (single anomaly over effective area)

To examine the characteristics of clusters that had a large change in the probability of burst, the points from Figure 12 were colored by attributes of the cluster. Figure 14 illustrates the results of the comparison plot where each cluster is colored by the number of anomalies in the cluster. Many anomalies with the highest probability of burst using the Single Anomaly method have 10 or more anomalies in the cluster. Note that any points on the plot that have more than 10 anomalies per cluster will be colored using the maximum of the color range (red in this Figure).

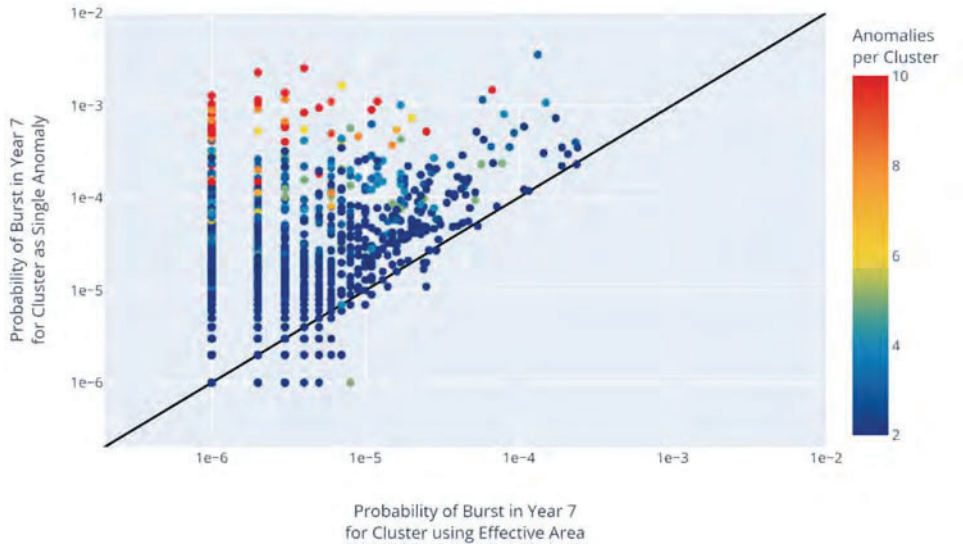

Figure 14. Comparison of probability of burst failure in Year 7, colored by anomalies per cluster

https://doi.org/10.52202/072781-0051

The same scatter plot as Figure 14 was colored by total cluster length in Figure 15. The color scale results in Figure 15 look similar to Figure 14 as overall cluster length was positively with the number of anomalies per cluster. In other words, clusters that had a high number of anomalies tended to also have a long overall cluster length, and these clusters generally saw a large decrease in the probability of burst failure when the Effective Area method was used instead of the Single Anomaly method. The same scatter plot was also colored by the maximum depth and is shown in Figure 16. Maximum depth was correlated to clusters that had a high probability of burst from both approaches; however, it did not correlate strongly to clusters that had a large decrease in the probability of burst failure when using the Effective Area method.

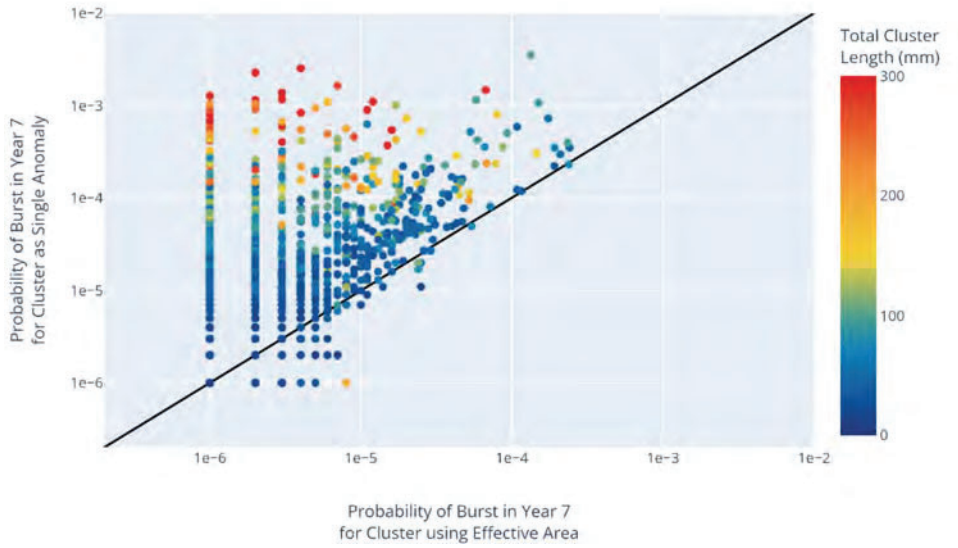

Figure 15. Comparison of probability of burst failure in Year 7, colored by total cluster length

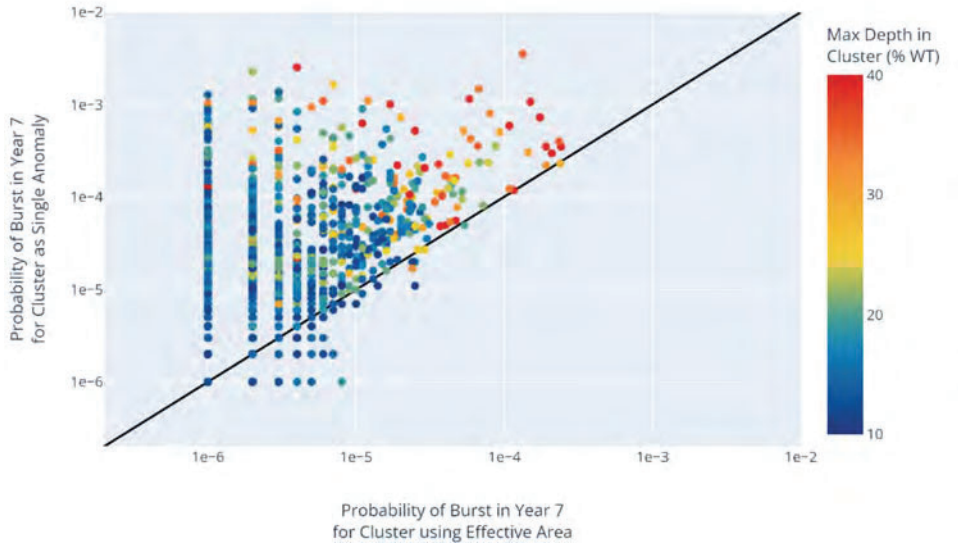

Figure 16. Comparison of probability of burst failure in Year 7, colored by max. depth in cluster

https://doi.org/10.52202/072781-0051

To consider both depth and length simultaneously, the aspect ratio was calculated as the ratio of the total cluster length over the maximum depth in the cluster, and the results are shown below in Figure 17. Clusters with a high aspect ratio were also correlated to a large decrease in the probability of burst failure (when moving from Single Anomaly to Effective Area). Clusters that are long with a high number of anomalies often contain mostly shallow features. A single moderately deep feature significantly increases the corroded area when using the Single Anomaly method relative to the Effective Area method.

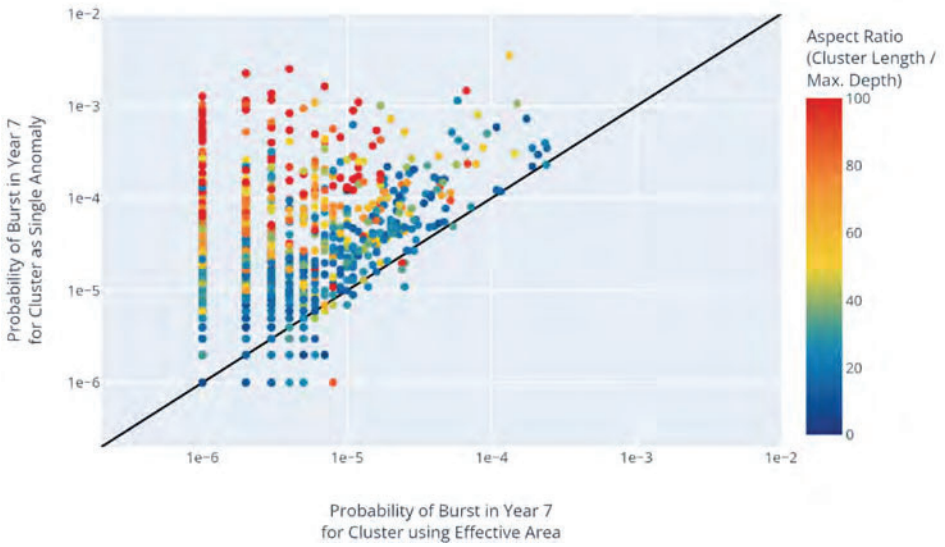

Figure 17. Comparison of probability of burst failure in Year 7, colored by aspect ratio

Implications for Integrity Management

To illustrate the impact that these two methods would have on a hypothetical integrity management program, the probability of failure results calculated for each cluster using each method were compared to the Ultimate Limit State (ULS) General Reliability targets from CSA Z662-23 Annex O [3]. If a hypothetical integrity management program used this reliability target as an intolerable limit where remediation was required for clusters that exceed the target, then the number of clusters requiring remediation can be calculated. The general reliability targets are calculated as:

$$R_T = \begin{cases} 1 - min\left(\frac{1600}{(PD^3)^{0.66}}, 10^{-3}\right) & for\ \rho = 0 \\ 1 - 10^{-3} & for\ 0 < \rho PD^3 \leq 6.0 \times 10^7 \\ 1 - \frac{6000}{\rho PD^3} & for\ \rho PD^3 > 6.0 \times 10^7 \end{cases} \quad (3)$$

where,

$\rho =$ The population density (people per hectare)

$P =$ The pressure (MPa)

$D =$ The diameter (mm)

https://doi.org/10.52202/072781-0051

Note that the reliability target in Equation 3 depends on the population density, pressure, and diameter of the pipeline. In an actual pipeline system, the reliability target would be calculated at the location of each cluster based on the specific pipeline properties (pressure, diameter) and surrounding population density. For simplicity of illustration in this study, all clusters were assumed to be found on an NPS16 (406.4 mm diameter) pipeline operating at 1200 psi (8.274 MPa), located in either a Class 1, 2, 3 or 4 location. The suggested population densities by Class Location from CSA Z662-23 Annex O were adopted [3].

When comparing the results to the reliability target, guidance in CSA Z662-23 Annex O allows for the probability of large leak to be pro-rated based on its smaller consequence (than rupture) before being added to probability of rupture. On this basis, the probability of equivalent rupture was calculated as:

$$p_{Equivalent\ Rupture} = p_{Large\ Leak} \cdot c_r + p_{Rupture} \quad (4)$$

where,

$p_{Large\ Leak}$ = The probability of large leak for a given cluster

c_r = The consequence ratio

$p_{Rupture}$ = The probability of rupture for a given cluster

Where the consequence ratio was calculated using the formula provided in CSA Z662-23 Annex O

$$c_r = \frac{7.5 \times 10^5}{D^3}, c_r \leq 1 \quad (5)$$

where,

D = The diameter (mm)

The results of the comparison between the probability of equivalent rupture results for each cluster and the reliability target for each method (Single Anomaly and Effective Area) are shown below in Figure 18. In a Class 1 area, the population density is low and therefore the required probability of equivalent rupture (at 1.0×10^{-3} per km-yr) is less restrictive than locations with a higher population density such as Class 2-4. If all of the clusters were located on the hypothetical pipeline (NPS 16, 1200 psi) in a Class 1 area, 18 of the clusters calculated using the Single Anomaly method would exceed the reliability target and require remediation. In comparison, none of the clusters calculated using the Effective Area method exceed the reliability target in a Class 1 area.

As the population density increases in a Class 2 location, the reliability target is more restrictive at 3.3×10^{-5} per km-yr. If all of the clusters were located in Class 2, 252 of the clusters evaluated using the Single Anomaly method would exceed the target, while only 2 of the clusters calculated using the Effective Area method would exceed the target.

https://doi.org/10.52202/072781-0051

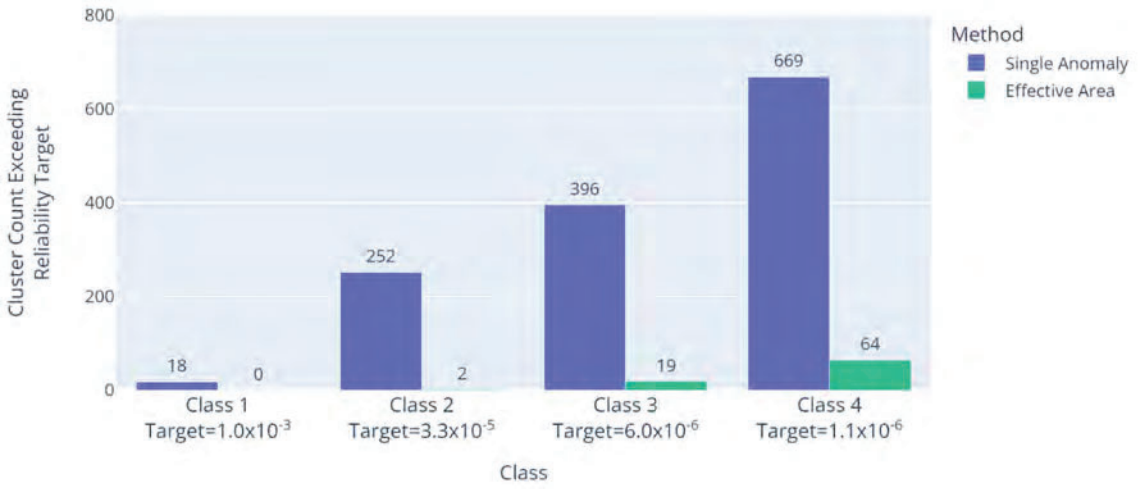

Figure 18. Count of clusters exceeding the CSA Z662 Annex O reliability target by method and class location

In Class 3 and 4 locations, the target continues to become more restrictive as the potential consequences increase due to increased population density. A count of 396 and 669 clusters evaluated using the Single Anomaly method exceed the target if they were located in Class 3 and Class 4 locations, respectively. In comparison, the Effective Area method only results in 19 and 64 clusters exceeding the reliability target. As this evaluation is illustrative, a detailed cost-benefit analysis was not conducted; however, it is evident that even a few avoided excavations would offset the additional engineering costs required to utilize the Effective Area method.

https://doi.org/10.52202/072781-0051

Summary

In this study, a collection of real-world corrosion clusters was simulated using two different methods: the Single Anomaly method and the Effective Area method. The Single Anomaly method models the clustered anomalies as a single anomaly that has the maximum depth associated with the deepest anomaly in the cluster, and a length equal to the total length of the cluster. The Effective Area method evaluates the profile created by the anomalies and determines the critical portion of the cluster by checking all possible combinations.

When using Direct Monte Carlo simulation to evaluate the probability of failure of the cluster, the Effective Area method increases the computation effort required by around 2 times for small clusters and more than 1000 times for large clusters (e.g. more than 100 anomalies in a cluster). As most clusters have a low number of anomalies, the total computational effort required to evaluate this dataset using the Effective Area method was 3 times more than the Single Anomaly method. The probability of burst failure results between the two methods ranged between a similar result to a reduction of around 3 orders of magnitude when using the Effective Area method. Clusters with the largest decrease in burst probabilities typically had a high number of anomalies, a large cluster length, and/or a high aspect ratio (Length/Max. Depth).

To illustrate the impacts these two methods would have on an integrity management program, the probability of failure results for the clusters were assumed to be found on a particular pipeline diameter and pressure, and assumed to be located in Class 1, 2, 3 or 4. More clusters exceed the reliability target using the Single Anomaly method than the Effective Area method in all cases, and as the target becomes more restrictive (e.g. Class 3 or 4), the Single Anomaly method results in hundreds of clusters exceeding the target while the Effective Area method only had only tens of clusters over the threshold.

These findings can be used by operators who utilize probabilistic corrosion analysis to evaluate the potential benefits of implementing the Effective Area method, which is a more computationally intensive analysis than the Single Anomaly method. In addition, these findings can guide operators developing probabilistic analysis programs to understand the implications of different assessment methodologies.

https://doi.org/10.52202/072781-0051

References

1. Transportation of Natural and Other Gas by Pipeline, 49 C.F.R. § 192 (2006).
2. Transportation of Hazardous Liquids by Pipeline, 49 C.F.R. § 195 (2006)
3. Canadian Standards Association. (2023). Oil and Gas Pipelines Systems. Canadian Standards Association, Ontario. CSA Z662-23, 2023.
4. PHMSA. (2022). General FAQs. Retrieved December 15, 2023. https://www.phmsa.dot.gov/faqs/general-faqs
5. PHMSA. (2022). Distribution, Transmission & Gathering, LNG, and Liquid Accident and Incident Data. Retrieved from https://www.phmsa.dot.gov/data-and-statistics/pipeline/distribution-transmission-gathering-lng-and-liquid-accident-and-incident-data.
6. PHMSA. (2020). Pipeline Risk Modeling: Overview of Methods and Tools for Improved Implementation. February 1, 2020.
7. Hong, H. P. (1997). Reliability Based Optimal Inspection And Maintenance For Pipeline Under Corrosion. Civil Engineering Systems, 14(4), 313–334.
8. Ahammed, M. (1998). Probabilistic estimation of remaining life of a pipeline in the presence of active corrosion anomalies. International Journal of Pressure Vessels and Piping, 75(4), 321–329.
9. Pandey, M. (1998). Probabilistic models for condition assessment of oil and gas pipelines. NDT & E International, 31(5), 349–358.
10. Det Norske Veritas. (1999). Recommended Practice for Corroded Pipelines. DNV-RP-F101, 1999.
11. Stephens, M., & Nessim, M. (2006). A Comprehensive Approach to Corrosion Management Based on Structural Reliability Methods. Proceedings of IPC 2006. 6th International Pipeline Conference. IPC2006-10458.
12. Zhang, S., and Zhou, W. (2012). An Efficient Methodology for the Reliability Analysis of Corroding Pipelines. Proceedings of the 2012 9th International Pipeline Conference. IPC2012-90482.
13. Bandstra, D., and Fraser, A. (2020). Subset Simulation for Structural Reliability Analysis of Pipeline Corrosion Anomalies. Proceedings of the 2020 13th International Pipeline Conference. IPC2020-9586.
14. Bandstra, D., Fraser, A., Rojas, J.S., and Dessein, T. (2022). Subset Simulation of Pipeline Corrosion, Crack, and Dent Anomalies Considering Multiple Limit States with Large-Scale Validation. Proceedings of the ASME 2022 13th International Pipeline Conference. IPC2022-87255.
15. Stephens, M., Nessim, M., & van Roodselaar, A. (2010). Reliability-Based Corrosion Management: The Impact of Maintenance and Implications for the Time to Next Inspection. Proceedings of the 8th International Pipeline Conference. IPC2010-31399.
16. Kariyawasam, S., & Peterson, W. (2010). Effective Improvements to Reliability Based Corrosion Management. In 2010 8th International Pipeline Conference. IPC2010-31425.
17. Zhou, W., & Huang, G. X. (2012). Model error assessments of burst capacity models for corroded pipelines. International Journal of Pressure Vessels and Piping, 99–100, 1–8.
18. ISO 16708. (2006). Petroleum and natural gas industries-Pipeline transportation systems-Reliability based limit state methods. First edition, Geneva, Switzerland.
19. Kiefner, J.F., and Vieth, P.H. (1989). A Modified Criterion for Evaluating the Remaining Strength of Corroded Pipe. Report to the Pipeline Corrosion Supervisory Committee of the Pipeline Research Committee of the American Gas Association. Project PR 3-805. Arlington, VA.

https://doi.org/10.52202/072781-0051

20. Kiefner, J. F., and Vieth, P. H., (1989). A Modified Criterion for Evaluating the Remaining Strength of Corroded Pipe. PRCI Report Catalog No. L 51609, Contract Catalog No. PR 3 805, Battelle Columbus Div., December 22, 1989.

https://doi.org/10.52202/072781-0051